Journal Pre-proof

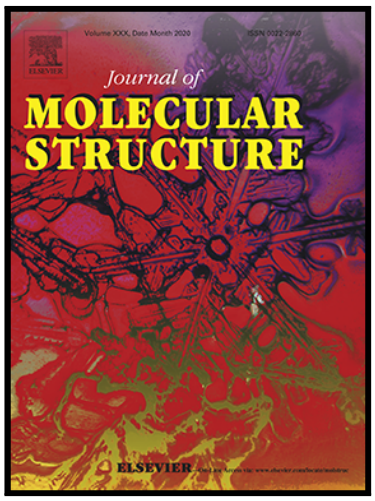

Synthesis of novel amides with antiradical capacity from 2-mercaptobenzimidazole and cinnamic acids: Evaluation through donor-acceptor maps and QSAR

Omar Alejandro Ramos Rodríguez , Juan Pablo Mojica Sánchez , José Antonio Valcárcel Gamiño , Fernando Obledo Benicio , Carlos Eduardo Macías Hernández , María Teresa Sumaya Martínez , Francisco J. Martínez Martínez , Zeferino Gómez Sandoval , Ángel Ramos-Organillo

PII: S0022-2860(20)31242-4
DOI: https://doi.org/10.1016/j.molstruc.2020.128917
Reference: MOLSTR 128917

To appear in: *Journal of Molecular Structure*

Received date: 22 May 2020
Revised date: 6 July 2020
Accepted date: 15 July 2020

Please cite this article as: Omar Alejandro Ramos Rodríguez , Juan Pablo Mojica Sánchez , José Antonio Valcárcel Gamiño , Fernando Obledo Benicio , Carlos Eduardo Macías Hernández , María Teresa Sumaya Martínez , Francisco J. Martínez Martínez , Zeferino Gómez Sandoval , Ángel Ramos-Organillo , Synthesis of novel amides with antiradical capacity from 2-mercaptobenzimidazole and cinnamic acids: Evaluation through donor-acceptor maps and QSAR, *Journal of Molecular Structure* (2020), doi: https://doi.org/10.1016/j.molstruc.2020.128917

This is a PDF file of an article that has undergone enhancements after acceptance, such as the addition of a cover page and metadata, and formatting for readability, but it is not yet the definitive version of record. This version will undergo additional copyediting, typesetting and review before it is published in its final form, but we are providing this version to give early visibility of the article. Please note that, during the production process, errors may be discovered which could affect the content, and all legal disclaimers that apply to the journal pertain.

© 2020 Published by Elsevier B.V.

Journal Pre-proof

Highlights

- Antioxidant activity, DAM, electrophilicity and QSAR of compounds were described.
- **MBZ** and **I-III** compounds showed high antioxidant activity.
- The results of DAM in DMSO phase are consistent of the antioxidant assays.
- The size and molecular shape are relevant for the antiradical activity.

Journal Pre-proof

Journal Pre-proof

Synthesis of novel amides with antiradical capacity from 2-mercaptobenzimidazole and cinnamic acids: Evaluation through donor-acceptor maps and QSAR

Omar Alejandro Ramos Rodríguez[a], Juan Pablo Mojica Sánchez[b], José Antonio Valcárcel Gamiño[c], Fernando Obledo Benicio[a], Carlos Eduardo Macías Hernández[a], María Teresa Sumaya Martínez[d], Francisco J. Martínez Martínez[a], Zeferino Gómez Sandoval[a], and Ángel Ramos-Organillo[a*]

[a] Facultad de Ciencias Químicas. Universidad de Colima, Km 9 Carretera Colima-Coquimatlán, Coquimatlán, Colima. C.P. 28400, México.

[b] Tecnológico Nacional de México. Instituto Tecnológico José Mario Molina Pasquel y Henríquez Campus Tamazula de Gordiano, Carretera Tamazula-Santa Rosa No. 329, Tamazula de Gordiano, Jalisco. C.P. 49650, México.

[c] Centro de Investigación en Dinámica Celular. Universidad Autónoma del Estado de Morelos, Avenida Universidad No. 1001, Chilapa, Cuernavaca, Morelos. C.P. 62210, México.

[d] Unidad de Tecnología de Alimentos. Universidad Autónoma de Nayarit, Cd. de la Cultura "Amado Nervo" Boulevard Tepic-Xalisco s/n, Tepic, Nayarit. C.P. 63190, México.

* Corresponding author: aaramos@ucol.mx

Journal Pre-proof

Abstract

The structures of thioethers **I-III** and the new amidic compounds **1**(**a-f**)-**3**(**a-f**) derived from 2-mercaptobenzimidazole (**MBZ**) and cinnamic acids were confirmed by NMR and elemental analysis. Antioxidant activity was evaluated by 1,1-diphenyl-2-picrylhydrazyl (DPPH●) radical scavenging assay and 2,2-azinobis (3-ethyl benzothiazoline-6-sulfonic acid) ABTS●+ radical cation decolorization method. Besides, donor-acceptor maps (DAM) and electrophilicity were calculated using DFT/B3LYP method with a 6-311G(d,p) basis set. **MBZ**, **I-III** and (**1a**-**3a)** compounds showed higher activity in *in vitro* antioxidant assays, confirming with *in silico* studies that they are the best candidates. The findings found in antiradical activity suggest that these compounds could be promising in the development of new antitumor and antimicrobial agents. QSAR Molecular properties and topological descriptors of the synthesized compounds **1(a-f)-3(a-f)** were calculated. The QSAR model indicates that the size and molecular shape are relevant for the antiradical activity for this family of compounds.

Keywords

Donor-Acceptor-Maps; DFT; Antiradical-capacity; 2-mercaptobenzimidazole-and-cinnamic acids-derivates; DPPH•; QSAR.

Introduction

In the search for new drugs for various pathologies, organic chemists have designed and synthesized heterocyclic compounds. Heterocyclic compounds are relevant in fields of medicine, biochemistry, environmental chemistry (herbicides and pesticides), coordination, and organometallic chemistry [1]. This type of compound is used as a nucleus to obtain

Journal Pre-proof

new functionalized compounds. The 2-mercaptobenzimidazole (**MBZ**) that has a thiol group in position-2 that has a tautomeric behavior, where it passes from the thiol to thione form and the reverse [2] (**Figure 1**). In the ^{1}H and ^{13}C NMR spectra for the **MBZ** molecule at room temperature show only three signals for ^{1}H and four signals for ^{13}C, which would not happen if the system did not have tautomeric equilibrium, as six signals would be expected for the ^{1}H and seven for the ^{13}C spectrum [3].

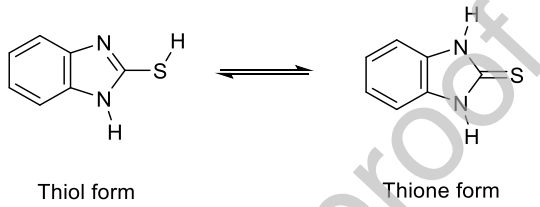

Figure 1. Tautomeric forms of 2-mercaptobenzimidazole (MBZ).

MBZ has pharmacological activity as antimicrobial [4], antihistamine, analgesic, anticonvulsant, neutropic [5], antioxidant [6, 7], and anti-ulcerative activities. The antiulcer drugs derived from 2-mercaptobenzimidazole are omeprazole, lansoprazole, rabeprazole, esomeprazole, which suppress gastric acid secretion by inhibiting the proton pump [8].

MBZ serves as a plant growth regulator and is also used in non-biological applications [9]. Also, it is widely used as an antioxidant for rubber and plastics [10], and some derivatives exhibit insecticidal properties [11]. It is also a well-known analytical reagent for mercury. It has been used for the determination of metallic ions Fe(II), Cu(II), and Cd(II) in sewage water and industrial wastewater samples [12, 13].

Journal Pre-proof

Different methods have determined the antioxidant activity of new benzimidazole derivatives: *in vitro* at the microsomal level of NADPH-dependent lipid peroxidation in rat liver, the scavenging of superoxide anion and the stable radical 2,2-diphenyl-1-picrylhydrazil (DPPH) [14]. It has been found that benzimidazole derivatives present an excellent antioxidant activity. The compounds 2-styryl-1H-benzimidazole, 2-(2-chlorostyryl)-1H-benzimidazole, and 2-(2-(1H-benzimidazole-2-yl)vinyl)phenol which shows an inhibition percentage higher than 90% at nitric oxide radical inhibition test, being more potent than ascorbic acid (reference antioxidant) [15].

There are different mechanisms by which phenolic antioxidants can scavenge free radicals: 1) electron transfer (ET), 2) hydrogen atom transfer (HAT), and 3) sequential proton loss electron transfer (SPLET) [16]. Although it is also true that there are mechanisms that explain the antioxidant activity and that are not related to free radicals. There are also non-chemical routes (enzymatic) [17]. In this sense, it is well known that ionization potential (**I**) and electron affinity (**A**) are properties of a system that can measure its propensity to donate or accept an electron. The best antioxidants have low **I** value, because the lower the value, the easier it is too abstract electrons, and *vice versa* for **A** to accept electrons (anti-reducer). It is valid provided that the electron transfer reaction is not located in the inverted zone of the Marcus parabola. Otherwise, lower values of ionization energy lead to prolonged reactions [18, 19].

There is now a model that explains the relative search activity and antioxidant power of the compounds that use these two properties [20]. Quantum chemical density functional theory (DFT) calculations can be used to obtain ionization potentials, electron affinities, electron-donation (**Rd**), and electron-acceptor (**Ra**) power indices (concerning the such as fluorine and sodium atoms). A plot of **Rd** *vs.* **Ra** can be used to construct a

donator acceptor map (DAM) **Figure 2**, indicating whether the molecules are good electron donator or acceptors.

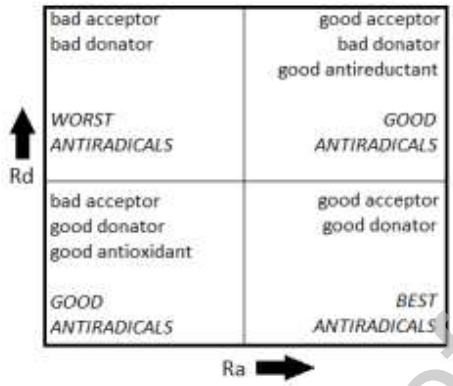

Figure 2. Donator acceptor map (**DAM**) [21-26].

The DAM is a representation of these properties (**Rd** *vs.* **Ra**), helping to exhibit the antiradical capacity of any substance and allowing qualitative comparison between substances [21]. Previous DAM studies by Ana Martínez have included linear polyene-conjugated molecules, an extensive series of carotenoids, melatonin, and vitamins, and psittacofulvine and anthocyanins which present a high antiradical capacity [21-26].

In the present study, a new series of amides **1(a-f)-3(a-f)** was synthesized using Neises & Steglich's reaction. The chemical structures were confirmed using ^{1}H-NMR, ^{13}C-NMR, IR, and elemental analysis. Besides, the antioxidant activity was calculated to find new amide derivatives with potential anticancer and antimicrobial activity.

Materials and methods

General experimental procedure

Journal Pre-proof

The reagents used (2-mercaptobenzimidazole, iodomethane, iodoethane, iodopropane, cinnamic acid derivatives, DCC, DMAP, silica gel 60 Å) were Sigma-Aldrich reagent grade and were used without extra purification. The three thioethers **I-III**, as well as the 18 synthesized amides **1(a-f)-3(a-f)**, were characterized by infrared spectroscopy techniques in a spectral range (4000-600 cm^{-1}) using a Varian 3100 FT-IR spectrometer of the Excalibur series. ^{1}H, ^{13}C NMR, were recorded in $CDCl_3$ or DMSO-d_6 using Bruker Ultra shield Plus 400 (^{1}H, 400; ^{13}C, 100.62 MHz). Data for ^{1}H NMR are reported as chemical shifts (δ ppm), multiplicity (s= singlet, d= doublet, q= quartet, m= multiple), integration, and assignment; data for ^{13}C NMR are reported as a chemical shift (δ ppm). Elemental analysis of compounds was performed on the Leco TruSpect Micro (C, H, N).

General procedure for the synthesis of thioethers (I-III)

In a ball flask (6.66 mmol) of 2-mercaptobenzimidazole was placed, 20 mL of dimethylformamide (DMF) was added as a solvent. It was placed in vigorous agitation at 0 °C. An aqueous solution (2 mL) of NaOH (6.66 mmol) was then added, and agitation continued at 0 °C for 30 minutes. Alkyl halide (6.66 mmol) was then added and allowed to react for 24 hours at room temperature (**Scheme 1**). TLC monitored the progress of the reaction. After completion of the reaction, the mixture was inactivated with the addition of 100 mL of cold water, in which compounds **I-III** were precipitated and isolated by filtration and drying. The products were characterized by corresponding spectroscopic data (IR, ^{1}H, and ^{13}C NMR).

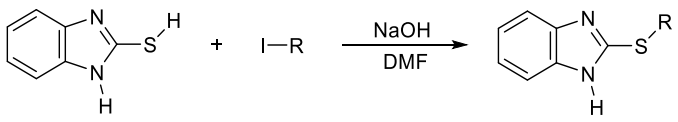

R= -CH_3 (**I**)
-CH_2CH_3 (**II**)
-$CH_2CH_2CH_3$ (**III**)

Journal Pre-proof

Scheme 1. Reaction to obtain thioethers **I-III**.

2-(methylthio)-1*H*-benzo[*d*]imidazole (I). White solid; yield 87% (0.95 g); m.p. 203-206 °C. IR (ν cm^{-1}): ν(N-H) 3117; ν(C=N) 1616; ν(C-N) 1346; δ(C-S) 663. ^{1}H NMR ($CDCl_3$, 400 MHz): δ (ppm) 7.28-7.23 (1H, m, H-5, H-6); 6.94-6.89 (2H, m, H-7, H-4); 2.52 (1H, s, H-11). ^{13}C NMR ($CDCl_3$, 100.62 MHz): δ (ppm) 151.9 (C2), 139.5 (C8), 139.5 (C9),

121.7 (C5), 121.7 (C6), 113.7 (C7), 113.7 (C4), 14.2 (C11). E.A $C_8H_8N_2S$ (%) Found: C (58.49), H (5.20), N (17.34); Calculated: C (58.10), H (4.91), N (17.06).

2-(ethylthio)-1*H*-benzo[*d*]imidazole (II). White solid; yield 81% (0.97 g); m.p. 171-174 °C. IR (ν cm^{-1}): ν(N-H) 3123; ν(C=N) 1616; ν(C-N) 1344; δ(C-S) 661. ^{1}H NMR ($CDCl_3$, 400 MHz): δ (ppm) 7.49-7.12 (4H, m, H-5, H-6, H-4, H-7); 3.27 (1H, c, H-11); 1.37 (1H, t, H-12). ^{13}C NMR ($CDCl_3$, 100.62 MHz): δ (ppm) 150.5 (C2), 121.8 (C8), 121.7 (C9), 117.7 (C5), 117.6 (C6), 111.1 (C4), 111.1 (C7), 26.3 (C11), 15.5 (C12). E.A $C_9H_{10}N_2S$ (%) Found: C (60.77), H (5.59), N (15.77); Calculated: C (60.64), H (5.65), N (15.72).

2-(propylthio)-1*H*-benzo[*d*]imidazole (III). White solid; yield 84% (1.08 g); m.p. 164-166 °C. IR (ν cm^{-1}): ν(N-H) 3121; ν(C=N) 1620; ν(C-N) 1344; δ(C-S) 673. ^{1}H NMR ($CDCl_3$, 400 MHz): δ (ppm) 7.44 (2H, m, H-4, H-7); 7.13 (2H, m, H-5, H-6); 3.24 (2H, t, H-18); 1.72 (2H, s, H-19); 0.98 (3H, t, H-20). ^{13}C NMR ($CDCl_3$, 100.62 MHz): δ (ppm) 147.1 (C2), 138.9 (C9, C8), 123.0 (C6, C5), 115.2 (C4, C7), 38.6 (C18), 21.6 (C19), 13.0 (C20). E.A $C_{10}H_{12}N_2S$ (%) Found: C (62.67), H (6.39), N (14.79); Calculated: C (62.47), H (6.29), N (14.57).

General procedure for the synthesis of amides 1(a-f)-3(a-f)

In a ball flask, **I-III** (1.83 mmol), (1.83 mmol) of the corresponding *trans*-cinnamic acid, and (0.183 mmol) of DMAP were added to 30 mL of dry DCM. These were kept in agitation at 0°C. Dropwise (1.83 mmol) of DCC previously dissolved in dry DCM was added. It was left at 0 °C for one hour and then left at room temperature for 24 hours (**Scheme 2**). The progress of the reaction was monitored by TLC. After completion of the reaction, the mixture was filtered to remove the DCU and then evaporated the solvent at reduced pressure. Compounds **1(a-f)-3(a-f)** were purified by the chromatographic column of silica gel (60 Å) at elution of 1:9 (ethyl acetate:hexane). The products were characterized by corresponding spectroscopic data (IR, ^{1}H, and ^{13}C NMR).

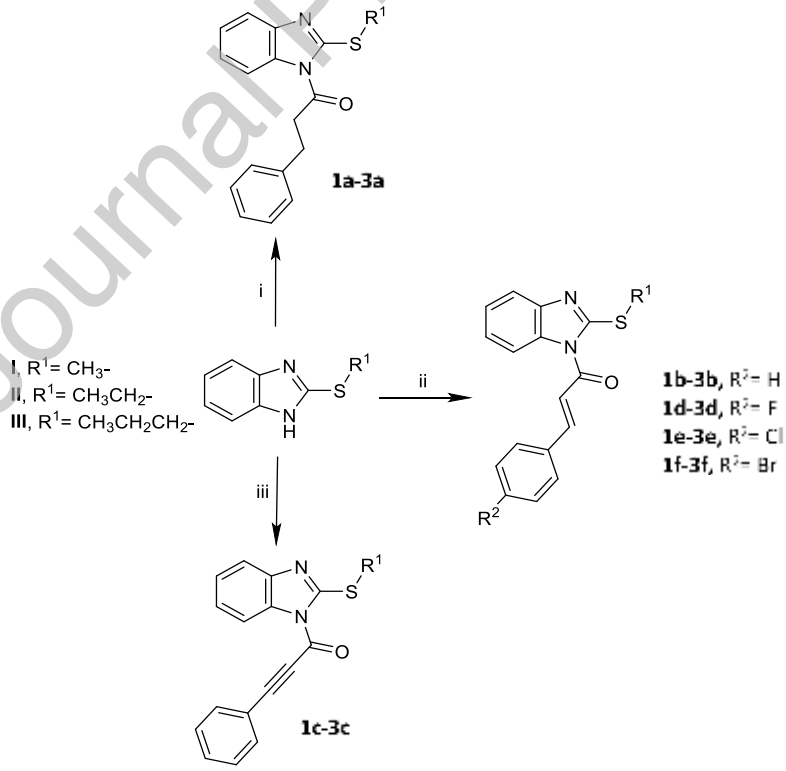

Journal Pre-proof

Scheme 2. Reaction to obtain of the compounds **1**(**a-f**)-**3**(**a-f**). (i) hydrocinnamic acid (**a**); (ii) *trans*-cinnamic acid (**b**), 4-fluoro *trans*-cinnamic acid (**d**), 4-chloro *trans*-cinnamic acid (**e**), 4-Bromo *trans*-cinnamic acid (**f**); (iii) phenylpropiolic acid (**c**).

1-(2-(methylthio)-1*H*-benzo[*d*]imidazol-1-yl)-3-phenylpropan-1-one (1a). Yellow solid; yield 49% (0.35 g); m.p. 43-46 °C. IR (ν cm^{-1}): ν(C=O) 1667; ν(C=C) 1625; ν(C=N) 1581; ν(C-N) 1327; δ(C-S) 667. ^{1}H NMR ($CDCl_3$, 400 MHz): δ (ppm) 7.87 (1H, m, H-7); 7.64 (1H, m, H-4); 7.34 (1H, m, H-5); 7.28 (2H, m, H-16); 7.23 (2H, m, H-15); 7.21 (1H, m, H-6); 2.95 (1H, d, H-13); 2.83 (2H, d, H-12); 2.57 (3H, s, H-18). ^{13}C NMR ($CDCl_3$, 100.62 MHz): δ (ppm) 170.3 (C11), 152.7 (C2), 148.3 (C9), 141.3 (C14), 132.1 (C8), 128.6 (C16), 127.7 (C15), 125.9 (C17), 123.5 (C6), 122.9 (C5), 119.6 (C4), 119.2 (C7), 36.4 (C12), 30.1 (C13), 14.5 (C18). E.A $C_{17}H_{16}N_2OS$ (%) Found: C (68.94), H (5.70), N (9.78); Calculated: C (68.89), H (5.44), N (9.45).

(E)-1-(2-(methylthio)-1*H*-benzo[*d*]imidazol-1-yl)-3-phenylprop-2-en-1-one (1b). Yellow solid; yield 40% (0.35 g); m.p. 119-121 °C. IR (ν cm^{-1}): ν(C=O) 1676; ν(C=C) 1612; ν(C=N) 1574; ν(C-N) 1330; δ(C-S) 669. ^{1}H NMR ($CDCl_3$, 400 MHz): δ (ppm) 7.94 (1H, d, H-13, *J=16 Hz*); 7.86 (1H, m, H-4); 7.70-7.64 (2H, m, H-7, H-16, H-17, H-21); 7.52-7.41 (2H, m, H-18, H-19, H-20); 7.51 (1H, d, H-14); 7.40-7.31 (2H, m, H-5, H-6); 2.67 (1H, s, H-11). ^{13}C NMR ($CDCl_3$, 100.62 MHz): δ (ppm) 164.8 (C12), 155.3 (C2), 147.9 (C9), 143.9 (C15), 134.4 (C16), 133.8 (C8), 131.7 (C19), 129.6 (C18, C20), 129.4 (C17, C21), 124.7 (C6), 123.9 (C5), 119.5 (C14), 118.7 (C4), 114.2 (C7), 15.9 (C11). E.A $C_{17}H_{14}N_2OS$ (%) Found: C (69.25), H (5.12), N (9.52); Calculated: C (69.36), H (4.79), N (9.52).

1-(2-(methylthio)-1*H*-benzo[*d*]imidazol-1-yl)-3-phenylprop-2-yn-1-one (1c). Yellow solid; yield 65% (0.35 g); m.p. 83-86 °C. IR (ν cm^{-1}): ν(C≡C) 2200; ν(C=O) 1668; ν(C=N) 1591; ν(C-N) 1330; δ(C-S) 673. ^{1}H NMR ($CDCl_3$, 400 MHz): δ (ppm) 8.26 (1H, m, H-7); 7.74 (1H, m, H-4); 7.65 (1H, m, H-6); 7.57 (1H, m, H-5); 7.50 (2H, m, H-15); 7.46 (1H, m, H-17); 7.31 (2H, m, H-16); 2.77 (3H, s, H-18). ^{13}C NMR ($CDCl_3$, 100.62 MHz): δ (ppm) 155.8 (C11), 149.3 (C2), 143.8 (C9), 133.0 (C15), 131.5 (C8), 128.6 (C16), 128.3 (C17), 125.2 (C5), 123.2 (C6), 119.5 (C14), 118.5 (C4), 113.8 (C7), 96.3 (C13), 82.8 (C12), 15.6 (C18). E.A $C_{17}H_{12}N_2OS$ (%) Found: C (69.84), H (4.46), N (9.67); Calculated: C (69.84), H (4.14), N (9.58).

(E)-3-(4-fluorophenyl)-1-(2-(methylthio)-1*H*-benzo[*d*]imidazol-1-yl)prop-2-en-1-one (1d). Yellow solid; yield 56 % (0.32 g); m.p. 138-12 °C. IR (ν cm^{-1}): ν(C=O) 1681; ν(C=C) 1622; ν(C=N) 1593; ν(C-N) 1328; δ(C-S) 673. ^{1}H NMR ($CDCl_3$, 400 MHz): δ (ppm) 7.96 (1H, d, H-13, *J=16 Hz*); 7.73 (2H, m, H-15), 7.69 (1H, m, H-4); 7.65 (1H, m, H-7); 7.35 (2H, m, H-16); 7.25 (2H, d, H-12, *J=16 Hz*); 7.2 (1H, m, H-5); 7.15 (1H, m, H-6); 2.8 (3H, s, H-18). ^{13}C NMR ($CDCl_3$, 100.62 MHz): δ (ppm) 164.5 (C11), 155.1 (C2), 147.1 (C13), 143.4 (C9), 133.5 (C14), 131.0 (C8), 130.8 (C7), 124.9 (C16), 124.8 (C15), 118.8 (C6), 118.2 (C12), 116.5 (C5), 116.4 (C4), 113.5 (C7), 16.0 (C18). E.A $C_{17}H_{13}FN_2OS$ (%) Found: C (65.21), H (4.37), N (9.14); Calculated: C (65.37), H (4.20), N (8.97).

(E)-3-(4-chlorophenyl)-1-(2-(methylthio)-1*H*-benzo[*d*]imidazol-1-yl)prop-2-en-1-one (1e). Yellow soli; yield 50 % (0.3 g); m.p. 152-154 °C. IR (ν cm^{-1}): ν(C=O) 1685; ν(C=C) 1625; ν(C=N) 1589; ν(C-N) 1329; δ(C-S) 667. ^{1}H NMR ($CDCl_3$, 400 MHz): δ (ppm) 7.8 (1H, d, H-13, *J=16 Hz*); 7.59 (2H, m, H-15), 7.53 (1H, m, H-4); 7.48 (1H, m, H-7); 7.32 (2H, m, H-16); 7.23 (1H, m, H-5); 7.18 (2H, d, H-12 *J=15.8 Hz*); 7.15 (1H, m, H-

Journal Pre-proof

6); 2.66 (3H, s, H-18). ^{13}C NMR ($CDCl_3$, 100.62 MHz): δ (ppm) 164.4 (C11), 155.1 (C2), 146.5 (C13), 143.5 (C9), 137.4 (C14), 133.8 (C8), 132.3 (C17), 129.8 (C16), 129.5 (C15), 124.7 (C6), 123.4 (C5), 118.9 (C12), 118.7 (C4), 113.4 (C7), 15.9 (C18). E.A $C_{17}H_{13}ClN_2OS$ (%) Found: C (62.15), H (4.32), N (8.80); Calculated: C (62.10), H (3.99), N (8.52).

(E)-3-(4-bromophenyl)-1-(2-(methylthio)-1*H*-benzo[*d*]imidazol-1-yl)prop-2-en-1-one (1f). Yellow solid; yield 50 % (0.34 g); m.p. 122-124 °C. IR (ν cm^{-1}): ν(C=O) 1672; ν(C=C) 1616; ν(C=N) 1587; ν(C-N) 1336; δ(C-S) 631. ^{1}H NMR ($CDCl_3$, 400 MHz): δ (ppm) 7.93 (1H, d, H-13, *J=16 Hz*); 7.73 (2H, m, H-15), 7.67 (1H, m, H-4); 7.62 (1H, m, H-7); 7.53 (2H, m, H-16); 7.36 (1H, m, H-5); 7.31 (2H, d, H-12, *J=16 Hz*); 7.28 (1H, m, H-6); 2.81 (3H, s, H-18). ^{13}C NMR ($CDCl_3$, 100.62 MHz): δ (ppm) 164.4 (C11), 155.4 (C2), 147.0 (C13), 143.3 (C9), 133.5 (C8), 132.9 (C14), 132.5 (C15), 130.0 (C16), 126.0 (C17), 124.7 (C6), 123.7 (C5), 119.0 (C12), 118.6 (C4), 113.4 (C7), 15.9 (C18). E.A $C_{17}H_{13}BrN_2OS$ (%) Found: C (54.65), H (3.83), N (7.71); Calculated: C (54.70), H (3.51), N (7.51).

1-(2-(ethylthio)-1*H*-benzo[*d*]imidazol-1-yl)-3-phenylpropan-1-one (2a). Yellow solid; yield 62%; m.p. 86-88 °C. IR (ν cm^{-1}): ν(C=O); ν(C=C); ν(C=N); ν(C-N); δ(C-S). ^{1}H NMR ($CDCl_3$, 400 MHz): δ (ppm) 7.67 (2H, m, H-4, H-7); 7.39-7.22 (5H, m, H-18, H-19, H-20, H-21, H-22, H-5, H-6); 3.39 (1H, c, H-11); 3.35 (1H, t, H-15); 3.21 (1H, t, H-16); 1.50 (1H, t, H-12). ^{13}C NMR ($CDCl_3$, 100.62 MHz): δ (ppm) 171.4 (C13), 155.3 (C2), 144.1 (C17), 139.9 (C9), 132.9 (C8), 128.8 (C19, C21), 128.5 (C18, C22), 126.6 (C20), 124.6 (C6), 123.4 (C5), 118.8 (C4), 113.7 (C7), 39.9 (C15), 30.0 (C16), 27.0 (C11), 13.7 (C12). E.A $C_{18}H_{18}N_2OS$ (%) Found: C (69.35), H (6.10), N (8.81); Calculated: C (69.65), H (5.85), N (9.02).

Journal Pre-proof

(E)-1-(2-(ethylthio)-1*H*-benzo[*d*]imidazol-1-yl)-3-phenylprop-2-en-1-one (2b). Yellow solid; yield 48 % (0.41 g); m.p. 94-96 °C. IR (ν cm^{-1}): ν(C=O) 1687; ν(C=C) 1627; ν(C=N) 1597; ν(C-N) 1327; δ(C-S) 644. ^{1}H NMR ($CDCl_3$, 400 MHz): δ (ppm) 7.94 (1H, d, H-13, *J=16 Hz*); 7.85 (1H, m, H-4); 7.70-7.63 (5H, m, H-7, H-15, H-16, H-17); 7.53 (1H, d, H-12, *J=16 Hz*); 7.34-7.27 (2H, m, H-5, 6); 3.29 (1H, c, H-18); 1.39 (1H, t, H-19). ^{13}C NMR ($CDCl_3$, 100.62 MHz): δ (ppm) 165.1 (C11), 154.3 (C2), 148.1 (C9), 144.2 (C13), 134.7 (C14), 133.8 (C8), 131.7 (C17), 129.6 (C16), 129.4 (C15), 124.8 (C6), 123.9 (C5), 120.1 (C12), 118.6 (C4), 114.3 (C7), 26.9 (C18), 14.6 (C19). E.A $C_{18}H_{16}N_2OS$ (%) Found: C (70.36), H (5.45), N (8.99); Calculated: C (70.10), H (5.23), N (9.08).

1-(2-(ethylthio)-1*H*-benzo[*d*]imidazol-1-yl)-3-phenylprop-2-yn-1-one (2c). Yellow solid; yield 58 % (0.3 g); m.p. 73-75 °C. IR (ν cm^{-1}): ν(C≡C) 2117; ν(C=O) 1712; ν(C=N) 1573; ν(C-N) 1342; δ(C-S) 638. ^{1}H NMR ($CDCl_3$, 400 MHz): δ (ppm) 8.29 (1H, m, H-7); 7.76 (1H, m, H-4); 7.67 (1H, m, H-6); 7.57 (1H, m, H-5); 7.50 (2H, m, H-15); 7.37 (1H, m, H-17); 7.31 (2H, m, H-16); 3.40 (2H, c, H-18); 1.52 (3H, t, H-19). ^{13}C NMR ($CDCl_3$, 100.62 MHz): δ (ppm) 154.9 (C11), 149.4 (C2), 143.7 (C9), 133.2 (C8), 133.0 (C15), 131.7 (C17), 128.9 (C16), 125.2 (C5), 123.7 (C6), 118.8 (C14), 118.6 (C4), 113.8 (C7), 96.2 (C13), 82.6 (C12), 26.9 (C18) 13.8 (C19). E.A $C_{18}H_{14}N_2OS$ (%) Found: C (70.85), H (4.92), N (9.40); Calculated: C (70.56), H (4.61), N (9.14).

(E)-1-(2-(ethylthio)-1*H*-benzo[*d*]imidazol-1-yl)-3-(4-fluorophen-yl)prop-2-en-1-one (2d). Yellow solid; yield 57 % (0.31 g); m.p. 119-121 °C. IR (ν cm^{-1}): ν(C=O) 1685; ν(C=C) 1620; ν(C=N) 1597; ν(C-N) 1334; δ(C-S) 637. ^{1}H NMR (DMSO-d_6, 400 MHz): δ (ppm) 7.95 (1H, d, H13, *J=16 Hz*), 7.93 (2H, m, H15), 7.68 (1H, m, H4), 7.62 (1H, m, H7), 7.31 (1H, m, H5), 7.45 (1H, d, H12, *J=16 Hz*), 7.34 (2H, m, H16), 7.29 (1H, m, H6), 3.28 (2H, c, H18), 1.38 (3H, t, H19). ^{13}C NMR (DMSO-d_6, 100.62 MHz): δ (ppm) 165.0 (C11),

Journal Pre-proof

153.7 (C2), 145.1 (C9), 143.5 (C13), 133.1 (C14), 131.5 (C8), 131.1 (C17), 130.6 (C16), 130.5 (C15), 124.2 (C6), 123.4 (C5), 119.0 (C12), 118.2 (C4), 113.8 (C7), 26.4 (C18), 14.1 (C19). E.A $C_{18}H_{15}FN_2OS$ (%) Found: C (66.57), H (4.65), N (8.54); Calculated: C (66.24), H (4.63), N (8.58).

(E)-3-(4-chlorophenyl)-1-(2-(ethylthio)-1*H*-benzo[*d*]imidazol-1-yl)prop-2-en-1-one (2e). Yellow solid; yield 56 % (0.32 g); m.p. 125-127 °C. IR (ν cm^{-1}): ν(C=O) 1679; ν(C=C) 1616; ν(C=N) 1593; ν(C-N) 1336; δ(C-S) 642. ^{1}H NMR (DMSO-d_6, 400 MHz): δ (ppm) 7.96 (1H, d, H13, *J=16 Hz*), 7.93 (2H, m, H15), 7.73 (1H, m, H4), 7.68 (1H, m, H7), 7.60 (2H, m, H16), 7.55 (1H, d, H12, *J=16 Hz*), 7.36 (1H, m, H5), 7.33 (1H, m, H6), 3.32 (2H, c, H18), 1.43 (3H, t, H19). ^{13}C NMR (DMSO-d_6, 100.62 MHz): δ (ppm) 164.5 (C11), 154.0 (C2), 145.9 (C9), 143.5 (C13), 135.9 (C14), 133.1 (C8), 132.9 (C17), 130.7 (C16), 129.2 (C15), 124.3 (C6), 123.4 (C5), 120.0 (C12), 118.2 (C4), 113.8 (C7), 26.4 (C18), 14.1 (C19). E.A $C_{18}H_{15}ClN_2OS$ (%) Found: C (63.35), H (4.78), N (8.42); Calculated: C (63.06), H (4.41), N (8.17).

(E)-3-(4-bromophenyl)-1-(2-(ethylthio)-1*H*-benzo[*d*]imidazol-1-yl)prop-2-en-1-one (2f). Yellow solid; yield 51 % (0.33 g); m.p. 135-137 °C. IR (ν cm^{-1}): ν(C=O) 1681; ν(C=C) 1616; ν(C=N) 1583; ν(C-N) 1332; δ(C-S) 632. ^{1}H NMR (DMSO-d_6, 400 MHz): δ (ppm) 7.92 (1H, d, H13, *J=16 Hz*), 7.81 (2H, m, H15), 7.70 (1H, m, H4), 7.69 (1H, m, H7), 7.63 (2H, m, H16), 7.52 (1H, d, H12, *J=16 Hz*), 7.31 (1H, m, H5), 7.26 (1H, m, H6), 3.29 (2H, c, H18), 1.39 (3H, t, H19). ^{13}C NMR (DMSO-d_6, 100.62 MHz): δ (ppm) 164.8 (C11), 153.9 (C2), 145.0 (C13), 143.6 (C9), 133.2 (C14), 133.1 (C8), 132.2 (C17), 130.9 (C16), 125.0 (C15), 124.2 (C6), 123.6 (C5), 120.0 (C12), 118.2 (C4), 113.7 (C7), 26.3 (C18), 14.1 (C19). E.A $C_{18}H_{15}BrN_2OS$ (%) Found: C (56.11), H (4.25), N (7.47); Calculated: C (55.82), H (3.90), N (7.23).

3-phenyl-1-(2-(propylthio)-1*H*-benzo[*d*]imidazol-1-yl)propan-1-one (3a). Yellow solid; yield 72% (0.4 g); m.p. 84-86 °C. IR (ν cm^{-1}): ν(C=O) 1685; ν(C=N) 1589; ν(C-N) 1334; δ(C-S) 651. ^{1}H NMR ($CDCl_3$, 400 MHz): δ (ppm) 7.69 (1H, m, H-7); 7.67 (1H, m, H-4); 7.39 (2H, m, H-16); 7.35 (1H, m, H-6); 7.32 (2H, m, H-15); 7.28 (1H, m, H-5); 7.23 (1H, m, H-17); 3.42 (1H, d, H-12); 3.35 (2H, t, H-18); 3.22 (1H, d, H-13); 1.88 (2H, m, H-19); 1.13 (3H, t, H-20). ^{13}C NMR ($CDCl_3$, 100.62 MHz): δ (ppm) 171.0 (C11), 155.4 (C2), 144.1 (C8), 139.9 (C14), 133.0 (C9), 128.7 (C16), 128.4 (C6), 126.5 (C5), 124.5 (C15), 123.3 (C17), 118.7 (C7), 113.7 (C4), 40.0 (C12), 34.6 (C18), 30.1 (C13), 21.7 (C19), 13.5 (C20). E.A $C_{19}H_{20}N_2OS$ (%) Found: C (70.12), H (6.48), N (8.78); Calculated: C (70.34), H (6.21), N (8.63).

(E)-3-phenyl-1-(2-(propylthio)-1*H*-benzo[*d*]imidazol-1-yl)prop-2-en-1-one (3b). Yellow solid; yield 60 % (0.3 g); m.p. 76-78 °C. IR (ν cm^{-1}): ν(C=O) 1689; ν(C=C) 1624; ν(C=N) 1589; ν(C-N) 1329; δ(C-S) 648. ^{1}H NMR (DMSO-d_6, 400 MHz): δ (ppm) 7.93 (1H, d, H-13, *J=16 Hz*); 7.85 (2H, m, H-15); 7.68 (1H, m, H-4); 7.63 (1H, m, H-7); 7.51 (2H, m, H-16); 7.50 (1H, m, H-17); 7.48 (1H, d, H-12, *J=16 Hz*); 7.31 (1H, m, H-5); 7.28 (1H, m, H-6); 3.27 (2H, t, H-18); 1.76 (2H, m, H-19); 1.01 (3H, t, H-20). ^{13}C NMR (DMSO-d_6, 100.62 MHz): δ (ppm) 164.4 (C11), 153.7 (C2), 147.2 (C13), 143.3 (C9), 133.8 (C14), 133.1 (C8), 131.0 (C17), 129.0 (C15), 128.75 (C16), 124.1 (C5), 123.1 (C6), 119.1 (C12), 118.1 (C7), 113.5 (C4), 33.6 (C18), 21.6 (C19), 13.0 (C20). E.A $C_{19}H_{18}N_2OS$ (%) Found: C (70.57), H (5.85), N (8.50); Calculated: C (70.78), H (5.63), N (8.69).

3-phenyl-1-(2-(propylthio)-1*H*-benzo[*d*]imidazol-1-yl)prop-2-yn-1-one (3c). Yellow solid; yield 62 % (0.31 g); m.p. 53-56 °C. IR (ν cm^{-1}): ν(C≡C) 2202; ν(C=O) 1664; ν(C=N) 1595; ν(C-N) 1332; δ(C-S) 630. ^{1}H NMR (DMSO-d_6, 400 MHz): δ (ppm) 8.16 (1H, m, H-7); 7.82 (1H, m, H-4); 7.80 (1H, m, H-6); 7.66 (1H, m, H-5); 7.56 (2H, m,

Journal Pre-proof

H-15); 7.35 (1H, m, H-17); 7.31 (2H, m, H-16); 3.25 (2H, t, H-18); 1.77 (2H, m, H-19); 1.02 (3H, t, H-20). ^{13}C NMR (DMSO-d_6, 100.62 MHz): δ (ppm) 154.7 (C11), 149.2 (C2), 143.7 (C9), 133.5 (C8), 133.1 (C15), 132.6 (C17), 129.7 (C16), 125.7 (C5), 124.9 (C6), 118.5 (C14), 118.7 (C4), 118.5 (C7), 95.8 (C13), 82.8 (C12), 34.3 (C18), 21.8 (C19), 13.0 (C20). E.A $C_{19}H_{16}N_2OS$ (%) Found: C (70.88), H (5.35), N (8.41); Calculated: C (71.22), H (5.03), N (8.74).

(E)-3-(4-fluorophenyl)-1-(2-(propylthio)-1*H*-benzo[*d*]imidazol-1-yl)prop-2-en-1-one (3d). Yellow solid; yield 59% (0.31 g); m.p. 96-99 °C. IR (ν cm^{-1}): ν(C=O) 1689; ν(C=C) 1622; ν(C=N) 1597; ν(C-N) 1330; δ(C-S) 650. ^{1}H NMR (DMSO-d_6, 400 MHz): δ (ppm) 7.94 (1H, d, H-13, *J=16 Hz*); 7.93 (2H, m, H-15); 7.68 (1H, m, H-4); 7.62 (1H, m, H-7); 7.44 (1H, d, H-12, *J=16 Hz*); 7.36 (2H, m, H-16); 7.33 (1H, m, H-17); 7.32 (1H, m, H-5); 7.29 (1H, m, H-6); 3.26 (2H, t, H-18); 1.76 (2H, m, H-19); 1.01 (3H, t, H-20). ^{13}C NMR (DMSO-d_6, 100.62 MHz): δ (ppm) 164.9 (C11), 154.3 (C2), 146.5 (C13), 143.8 (C9), 133.7 (C8), 131.9 (C15), 131.0 (C14), 124.7 (C5), 123.9 (C6), 119.5 (C12), 118.7 (C7), 116.7 (C16), 116.5 (C17), 114.1 (C4), 33.9 (C18), 22.0 (C19), 13.6 (C20). E.A $C_{19}H_{17}FN_2OS$ (%) Found: C (67.34), H (5.31), N (8.17); Calculated: C (67.04), H (5.03), N (8.23).

(E)-3-(4-chlorophenyl)-1-(2-(propylthio)-1*H*-benzo[*d*]imidazol-1-yl)prop-2-en-1-one (3e). Yellow solid; yield 61 % (0.34 g); m.p. 138-140 °C. IR (ν cm^{-1}): ν(C=O) 1681; ν(C=C) 1618; ν(C=N) 1587; ν(C-N) 1331; δ(C-S) 644. ^{13}C NMR (solids): δ (ppm) 164.1 (C11), 156.8 (C2), 146.4 (C13), 136.0 (C9), 134.3 (C8), 128.3 (C15), 138.4 (C14), 126.0 (C5), 122.7 (C6), 121.0 (C12), 116.0 (C7), 129.7 (C16), 131.8 (C17), 113.4 (C4), 34.1 (C18), 21.5 (C19), 14.4 (C20). E.A $C_{19}H_{17}ClN_2OS$ (%) Found: C (64.28), H (5.12), N (8.14); Calculated: C (63.95), H (4.80), N (7.85).

(E)-3-(4-bromophenyl)-1-(2-(propylthio)-1*H*-benzo[*d*]imidazol-1-yl)prop-2-en-1-one (3f). Yellow solid; yield 55 % (0.32 g); m.p. 142-145 °C. IR (ν cm^{-1}): ν(C=O) 1683; ν(C=C) 1618; ν(C=N) 1583; ν(C-N) 1332; δ(C-S) 632. ^{13}C NMR (solids): δ (ppm) 164.4 (C11), 157.0 (C2), 146.5 (C13), 136.4 (C9), 132.1 (C8), 127.2 (C15), 135.8 (C14), 125.5 (C5), 123.0 (C6), 121.0 (C12), 116.6 (C7), 126.7 (C16), 130.4 (C17), 113.1 (C4), 34.3 (C18), 22.0 (C19), 13.9 (C20). E.A $C_{19}H_{17}BrN_2OS$ (%) Found: C (57.18), H (4.39), N (7.31); Calculated: C (56.86), H (4.27), N (6.98).

Antioxidant activity

The synthesized compound **III** was screened for their antioxidant activity by 1,1-diphenyl-2-picrylhydrazyl (DPPH●) radical scavenging assay and 2,2-azinobis (3-ethyl benzothiazoline-6-sulfonic acid) ABTS$^{\bullet+}$ radical cation decolorization method.

A Power wave XS microplates reader from biotek were used to read the absorbancies. Micropipettes (Thermofisher 89 finnpippete) of different capacities (25, 200, 1000 µL) were also used to prepare the required solutions. Eppendorf tubes (1 mL) were used for sample preparation. All tests were carried out in triplicate. For each run of samples a standard curve was made using the reference antioxidant in order to calculate the equivalents per mL of the reference antioxidant [27].

DPPH$^{\bullet}$ method

A solution of DPPH$^{\bullet}$ (7.4 mg/100 mL) was prepared and kept in the dark to avoid photodegradation. 50 µL were taken from a DMSO solution of compound **III** or the reference antioxidant (trolox) to which 250 µL of DPPH$^{\bullet}$ solution was immediately added.

The mixture was stirred vigorously with a microvortex and left it to stand at room temperature for one hour, then the absorbance was measured at 520 nm. The results of anti-radical activity were expressed as a percentage of inhibition and on µmol trolox/L equivalents (µmol TE/L) [28-29].

$ABTS^{\bullet+}$ method

The radical $ABTS^{\bullet+}$ was obtained by reacting $NH_4^+ABTS^{2-}$ (7mM) with potassium persulphate (2.45 mM) for 16 hours at 4 ºC in the dark. Once formed, the radical $ABTS^{\bullet+}$ was diluted with ethanol to obtain absorbance value of 0.70 (±0.1) at 754 nm. In an eppendorf tube 490 µL of the diluted solution of free radicals ($ABTS^{\bullet+}$) and 10 µL of the compounds to be analyzed or vitamin C (reference antioxidant) were added, the mixture was agitated vigorously and then 200 µL of this mixture were taken and its absorbance was read at 754 nm in a microplates reader. The results of anti-radical activity were expressed as a percentage of inhibition and in milligrams ascorbic acid equivalents per liter (mg AAE/L) [27-28].

Computational details

Geometry optimizations without symmetry restrictions in the gas phase were carried out for 26 structures within the framework of the density functional theory in the Gaussian 09 code [30]. For the exchange, a Becke's 1988 [31] formalism was used, and for the correlation, a Perdew and Wang's 1991 [32] functional was employed. The 6-311G (d, p) basis set [33] was utilized to describe all electrons, and frequency analysis was performed in order to verify the stationary points.

Journal Pre-proof

Once the minima energy geometry of each system has been established, anionic and cationic states were calculated by adding the negative and the positive charge, respectively, in the form of single points [34-35].

On the other hand, calculations in solutions were made using the optimized geometries and utilizing the SMD model [36] under the same level theory, and specifically, three solvents were considered: water, DMSO, and pentyl ethanoate. In all solvent cases, single points were effectuated to obtain energies for neutral, anionic, and cationic states. All calculations were realized in Gaussian 09 [29].

The ionization potential (**I**) was calculated using the difference between the energy of cation less the energy of neutral state, and the reduction capacity was estimated from the electron affinity (**A**) and calculated how the difference between the energy of neutral stateless the energy of anion. It is to evaluate the oxidant capacity of the molecules [37].

One tool that allows the measurement of the propensity to donate charge is called electron-donation power [20], which was defined as (**Equation 1**).

$$\omega^{-} = \frac{(\boldsymbol{3I + A})^{\boldsymbol{2}}}{\boldsymbol{16(I - A)}}$$

Equation 1.

Whereas the tool to describe the propensity to accept the charge or called electron-acceptor power [20], was defined as (**Equation 2**).

$$\omega^{+} = \frac{(\boldsymbol{I + 3A})^{\boldsymbol{2}}}{\boldsymbol{16(I - A)}}$$

Equation 2.

Journal Pre-proof

The ω^- and ω^+ were calculated for 26 molecules, and as a measure of comparison, it was estimated the ω^- of Na atom and the $\omega^+$of F atom. It is because Na represents a suitable electron donor, and F represents an excellent electron acceptor. For any molecule, it was defined as an electron acceptance index as (**Equation 3**).

$$\boldsymbol{R_a = \frac{\omega^+}{\omega_F^+}}$$

Equation 3.

Moreover, an electron donation index was defined as (**Equation 4**).

$$\boldsymbol{R_d = \frac{\omega^-}{\omega_{Na}^-}}$$

Equation 4.

If R_d=1, the molecule is an excellent electron donor as Na; if R_d<1, the molecule is better electron donor than Na and finally if R_d>1 is a poorer electron donor than Na. Besides, if R_a=1, the molecule is a suitable electron acceptor as F; if R_a<1 is a poorer electron acceptor than F and if R_a>1 is a better electron acceptor than F.

With the above information, it is possible to correlate the values of $\boldsymbol{R_a}$ and $\boldsymbol{R_d}$ of the molecules in the form of graphs called donor-acceptor maps [21-25]. A donor-acceptor map was created and was compared to the results of the novel amides compounds with known antioxidants substances: vitamin C, Trolox, Resveratrol, and Quercetin. Additionally, the calculations of electrophilicity were carried out, and it is defined as infinite differences as [38] (**Equation 5**).

$$\boldsymbol{\omega = \frac{(I+A)^2}{8(I-A)}}$$

Equation 5.

Journal Pre-proof

Results and discussion

Synthesis

The synthesis scheme consisted of two stages leading to the formation of a variety of amides **1(a-f)-3(a-f)**; the first was the formation of thioethers **I-III** from 2-mercaptobenzimidazole with alkyl halides in basic medium with yields of 90% after precipitation in cold water (**Scheme 1**). The second stage was the synthesis of the 18 new amidic compounds **1(a-f)-3(a-f)** (**Scheme 2**), using the N,N'-dicyclohexylcarbodiimide (DCC) methodology proposed by Neises & Steglich (1978) [39]. In which the thioethers **I-III** were reacted with the different derivatives of cinnamic acid (**a-f**) in an equimolar relationship using dry dichloromethane as the solvent, 4-(dimethylamino)pyridine (DMAP) as catalyst and N,N'-dicyclohexylcarbodiimide (DCC) as an activator of carboxylic acid towards substitution. Amides **1(a-f)-3(a-f)** were obtained with yields of 40-72% after column chromatography.

Structural elucidation of compounds I-III, 1(a-f)-3(a-f)

In ^{1}H NMR spectra for thioethers **I-III,** a broad singlet signal resonated at 8.5 ppm was assigned to the N-H of the imidazole ring. The amplitude of the signal is caused by the fast exchange of the proton with the other N present in the imidazole ring, caused by the tautomeric effect, which is faster than the resonance time scale. In spectra of the compounds (**1-3)(b**, **d**, **e**, **f**) two doublets were observed between the regions of 7.18-7.51 and 7.80-7.94 ppm due to H12 and H13 of the double bond of the *trans*-cinnamic acid

fragment, coupling constant (^{3}J(H12-H13)) was 16 Hz indicating the *trans*- position of the double bond.

In ^{13}C NMR of compounds **1**(**a-f**)-**3**(**a-f**), the signals between 171.1 and 154.7 ppm were assigned to carbonyl (C11). Where in **1**(**a-c**)-**3**(**a-c**) compounds there is an unprotected phenomenon this is due to the diamagnetic anisotropy present in the double and triple bond, the effect of this phenomenon can also be seen in the C2 signal where **1a-3a** derivatives appear at 155.7 ppm, **1b-3b** at 155.1 ppm and **1c-3c** at 149.3 ppm. (The NMR spectra are shown in the supplementary material).

Antioxidant activity

Table 1 shows the percentages of scavenging activity and antiradical activity in DPPH$^{\bullet}$ and ABTS$^{\bullet+}$. In the DPPH$^{\bullet}$ assay, the **MBZ** was able to capture 73% of the radical DPPH$^{\bullet}$, also showing better radical entrapment than the Trolox (reference antioxidant), showing 70%. Thioether **I** inhibition percentage of 26%, while **1a** presented 23%, **1c** trapped only 15%, compound **1f** inhibiting 46%, thioether **II** showed 18%, **2b** presented the lowest percentage with 12%, while **3c** showed a low percentage 26%.

Table 1. Antioxidant activity of MBZ and synthesized compounds.

Comp.	DPPH$^{\bullet}$		ABTS$^{\bullet+}$	
	% Scavenging	µmol TE/L	% Scavenging	mg AAE/L
MBZ	73 ± 0.59	325 ± 2.3	88 ± 2.68	27 ± 1.00
I	26 ± 2.05	77 ± 3.6	27 ± 7.80	8 ± 2.89
II	18 ± 1.20	36 ± 10.7	14 ± 5.54	4 ± 2.08
III	3 ± 1.86	5 ± 0.6	6 ± 4.44	1 ± 1.53
1a	23 ± 1.57	60 ± 4.2	4 ± 5.24	2 ± 1.15

1b	6 ± 2.77	**N/F	5 ± 3.32	**N/F
1c	15 ± 0.70	19 ± 3.6	4 ± 2.66	**N/F
1d	1 ± 1.97	**N/F	3 ± 3.59	**N/F
1e	1 ± 1.08	**N/F	3 ± 3.62	**N/F
1f	46 ± 1.56	184 ± 5.3	5 ± 4.11	**N/F
2a	9 ± 0.74	**N/F	8 ± 1.70	2 ± 1.00
2b	12 ± 1.28	4 ± 10.6	6 ± 1.34	**N/F
2c	5 ± 4.30	**N/F	5 ± 2.29	**N/F
2d	6 ± 1.10	**N/F	3 ± 5.31	**N/F
2e	1 ± 3.69	**N/F	2 ± 3.45	**N/F
2f	1 ± 2.92	**N/F	11 ± 4.54	3 ± 1.53
3a	9 ± 4.90	**N/F	5 ± 6.88	**N/F
3b	1 ± 2.62	**N/F	3 ± 4.04	**N/F
3c	26 ± 2.30	80 ± 8.7	5 ± 3.09	**N/F
3d	1 ± 0.35	**N/F	2 ± 2.72	**N/F
3e	*N/C	*N/C	*N/C	*N/C
3f	*N/C	*N/C	*N/C	*N/C
Trolox	70 ± 0.35	---	---	---
A. A	---	---	98 ± 0.34	---

*****N/C (Not calculated) Insoluble;
******N/F (Not found)

Journal Pre-proof

Only compounds **I**, **1a**, **1f**, and **3c** showed significant antiradical activity DPPH● ($p < 0.05$) concerning the target. 2-mercaptobenzimidazole (**MBZ**) showed significantly elevated antiradical activity (325 µmol ET/L). The compound **1f** presented the highest antiradical activity (184 µmol ET/L) followed by **3c** and thioether **I**, which presented the

activity of 80 and 77 µmol ET/L respectively. This difference in antiradical activity DPPH● between the amide compounds, thioethers (synthetic intermediates) and **MBZ** (raw material) may be due to substitution of the two active **MBZ** sites, on the one hand, the alkyl substitute in exocyclic sulfur, and the substitute (cinnamic derivative) in N1 to form the corresponding amides.

To explain the results is necessary to know that two known mechanisms can reduce the radical DPPH: HAT (Hydrogen Atom Transference) and ET (electron transference) [40]. There are differences between the authors, as some define it as an ideal radical for the ET measurement method, while others classify it for the HAT method. However, it is necessary to consider the structural characteristics of the antioxidant used [41]. In this assay of antioxidant activity, the mechanism of HAT can better explain the obtained results.

Journal Pre-proof

For the transfer mechanism of a hydrogen atom to occur, the dissociation energies of the N-H and S-H bonds must be considered. Data of the energies of dissociation of the N-H bond can be calculated much scarcer for aromatic amines [42], it is known that the

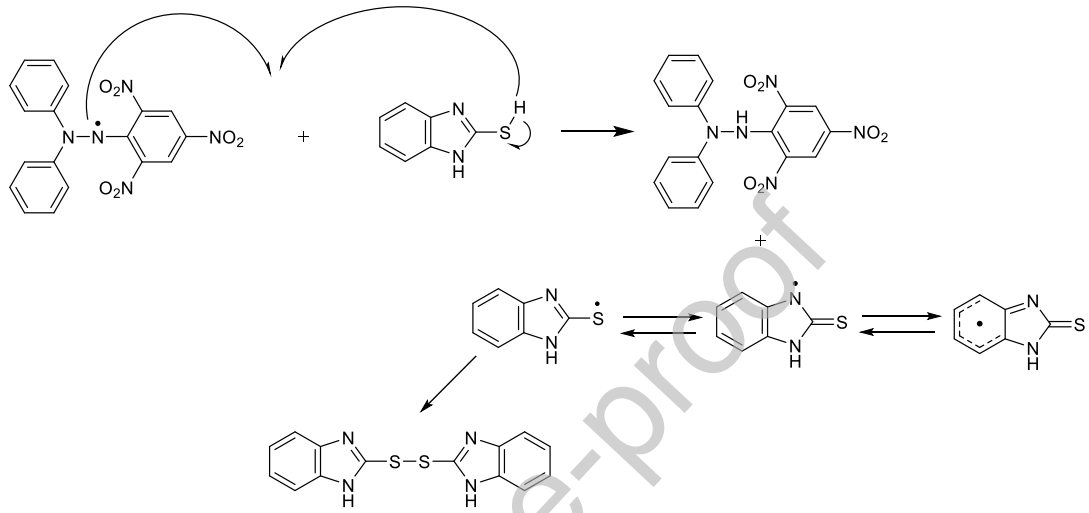

energy of this bond is higher than that of the S-H. It explains why the MBZ presented high antiradical activity compared to thioether derivatives **I**, **II**, and **III**, in which the S-H bond no longer exists, thus making it impossible to maintain the stability of the newly formed radical. The Sulfhydryl group is a crucial piece in the stability, either by retaining the charge or building disulfide bridges, thus neutralizing the free radical [43] (**Scheme 3**). Additionally, **Figure 3** presents the frontier orbitals of the systems with the highest antiradical capacity. It is essential to highlight that the areas with the highest energy levels occupied and the lowest energy levels unoccupied are mostly concentrated on the MBZ ring except for **2a** and **3a** compounds in the case of LUMO-type orbital.

Journal Pre-proof

Scheme 3. Mechanism of the antioxidant activity and stabilization of the **MBZ** against DPPH$^{\bullet}$.

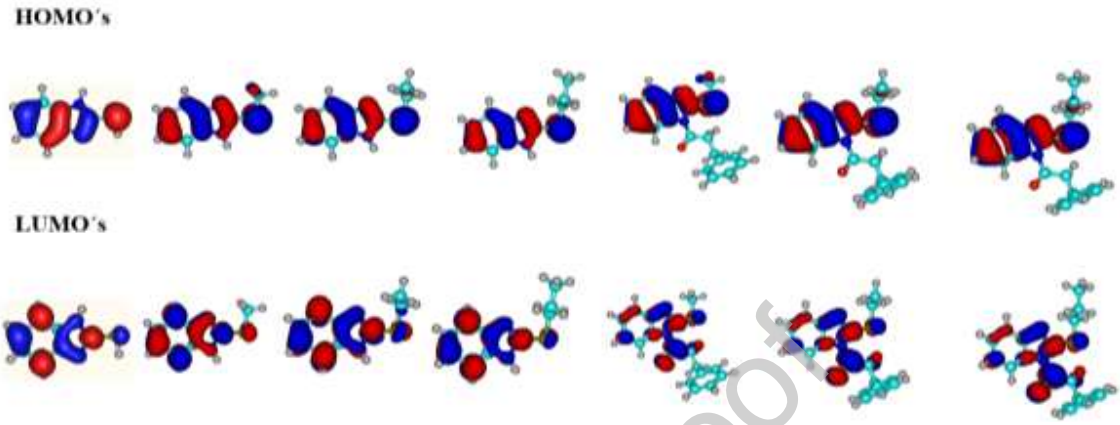

Figure 3. Frontier molecular orbitals of the compounds that showed higher activity in *in vitro* antioxidant assays. From left to right **MBZ, I, II, III, 1a, 2a,** and **3a.**

According to Barbuceanu *et al*. (2014) [44], the S-alkyl compounds derived from 1,2,4-triazoles showed an inhibitory effect in the antiradical activity DPPH$^{\bullet}$ proposing that the increase of the chain of alkyl substitution in sulfur and with it the increase of lipophilicity (>Log P) directly affects in the decrease of the antioxidant activity. This effect can be observed in the tendency of the antiradical activity of the compounds evaluated **I** (26%), **II** (18%) and **III** (3%) is that as the S-alkyl chain is lengthened, the antioxidant activity is considerably reduced.

In the trial ABTS$^{\bullet+}$ synthetic intermediates (thioethers) **I-III** presented the best radical entrapments, being **I** the one that presented the highest percentage (27%), followed by intermediary **II** with 14% and thioether **III** with 11%. **MBZ** presented a very high antiradical activity (88%) very close to that presented to the reference antioxidant (ascorbic acid). On the other hand, amide derivatives **1(a-f)-3(a-f)** presented low values of radical entrapment (from 2 to 6%). However, they do not present a significant difference

concerning the negative reference. The compounds **I** and **II** presented values with significant differences for the target, with 8 and 4 mg AAE/L (Ascorbic Acid Equivalents), respectively, **MBZ** presented the highest antiradical activity (27 mg AAE/L). The data confirm the trend seen in the assay by $DPPH^{\bullet}$, that the presence of the substitute in the exocyclic sulfur and the lengthening of the chain thus increasing the lipophilicity of the compound, causes a significant reduction of the antiradical activity.

The $ABTS^{\bullet+}$ method is considered an ET method, although the chemical characteristics of the antioxidant to be evaluated must be considered since these characteristics have a direct influence on the most favored mechanism [45]. The mechanism can also be influenced by the pH of the $ABTS^{\bullet+}$ solution, since ethanol has a pH of 7.4, where an alkaline pH is preferred to the ET mechanism, due to the chemical characteristics of $ABTS^{\bullet+}$ can be adapted to measure the antiradical activity of hydrophilic and lipophilic compounds in media with different pH [46, 41]. DMSO was the measuring solvent in this assay due to the insolubility compounds.

Donor Acceptor Map (DAM)

The DAM in different phases (gas, water, DMSO and pentyl ethanoate) were calculated for **MBZ**-derived compounds (thioethers and amides). The DAM are shown in **Figure 4(a-d)**. Water is the dominant solvent in living organisms, DMSO is the solvent utilized for *in vitro* tests of antiradical activities with $DPPH^{\bullet}$ and $ABTS^{\bullet+,}$ and pentyl ethanoate simulates the lipid shell of cell membranes.

Journal Pre-proof

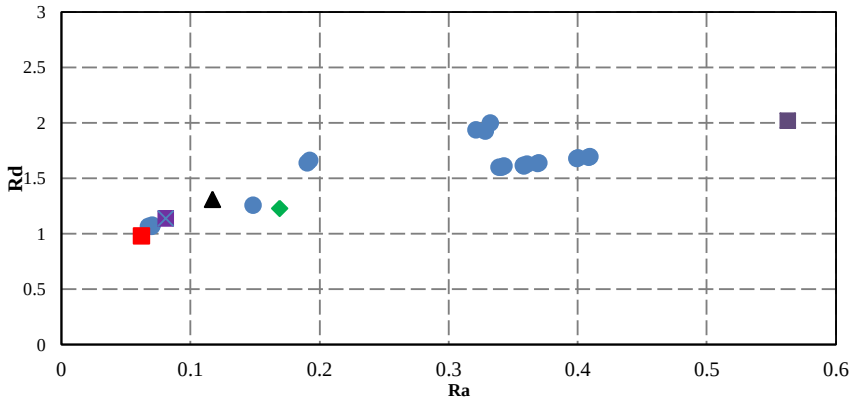

(a)

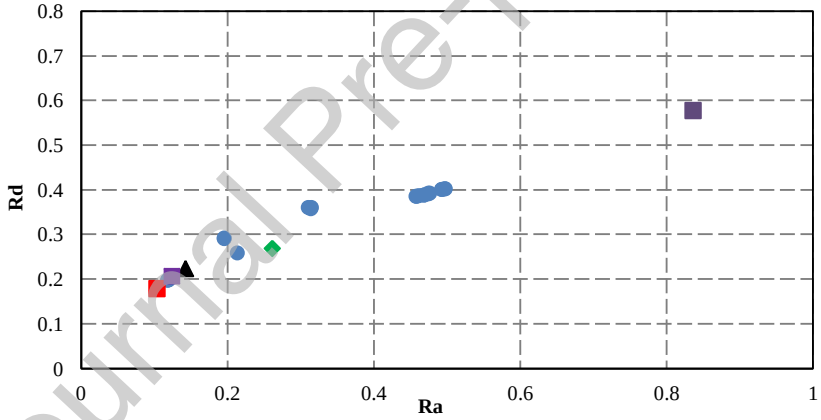

(b)

Journal Pre-proof

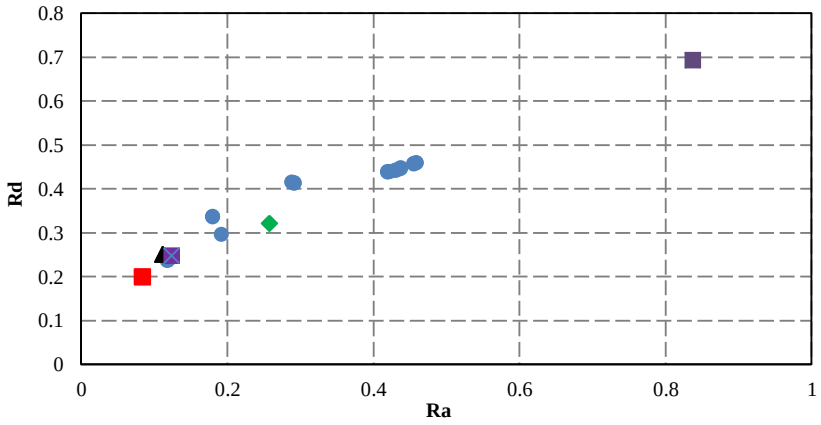

(**c**)

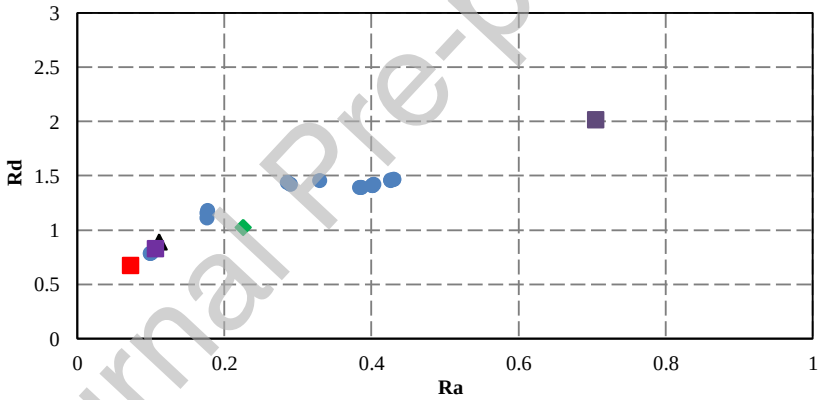

(**d**)

Figure 4. Donor Acceptor Maps in gas (**a**), water (**b**), DMSO (**c**) and pentylethanoate (**d**) phase for compounds **I-III**, **1(a-f)-3(a-f)**( ) and **MBZ** ( ). Antioxidants of reference: trolox ( ), ascorbic acid ( ), resveratrol ( ) and quercetin ( ).

In the gas-phase, MAD (**Figure 4a**, **Table 2**) for the study compounds, as well as the reference antioxidants (Vitamin C, Trolox, Resveratrol, and Quercetin) included for comparison. It shows that the evaluated compounds that present unsaturation and triple

bonds in the cinnamic acid fragment **1(b-f)-3(b-f)** have an increase in anti-reducing capacity, as does the antiradical Quercetin, being suitable acceptors of electrons. While compounds with saturated chains in the cinnamic acid fragment (**1a-3a**) are found in the region of worst antiradical, the smaller molecules (**MBZ** and thioethers **I-III**) and the reference antioxidants used (Vitamin C, Trolox, and Resveratrol) belong to the right antioxidant sector. The presence of alkyl chains does not affect antiradical behavior. However, the presence of the cinnamic acid fragment increases the anti-reducing capacity and decreases the antioxidant capacity. It is following the study carried out by Martínez in 2009 [25**]**, in which she proposes that the number of conjugated carbon atoms increases the anti-reducing capacity. However, the antioxidant capacity decreases. Large molecules fall within the right anti-reducer zone, while small molecules belong to the good antioxidant sector.

Table 2. Molecular descriptors calculated to obtain the donor-acceptor character (gas phase).

Comp.	I	A	ω^-	ω^+	R_a	R_d
I	172.789	-13.475	85.536	5.879	0.071	1.075
II	171.445	-13.996	84.373	5.648	0.068	1.060
III	170.430	-13.164	84.470	5.837	0.070	1.062
1a	170.686	3.709	99.570	12.373	0.149	1.251
1b	168.917	29.823	129.369	29.999	0.361	1.626
1c	171.145	28.079	128.104	28.492	0.343	1.610
1d	231.946	22.423	153.891	26.706	0.322	1.934
1e	238.954	23.285	158.756	27.636	0.333	1.995
1f	227.571	23.617	152.884	27.290	0.329	1.921
2a	224.997	3.905	130.291	15.840	0.191	1.637
2b	167.653	29.548	128.328	29.727	0.358	1.613
2c	169.775	27.771	126.964	28.192	0.340	1.596

Journal Pre-proof

2d	168.354	30.645	130.248	30.748	0.371	1.637
2e	167.820	33.274	133.822	33.275	0.401	1.682
2f	167.244	34.040	134.686	34.044	0.410	1.693
3a	227.896	3.902	131.917	16.018	0.193	1.658
3b	167.020	29.604	128.080	29.768	0.359	1.610
3c	169.055	27.982	126.876	28.358	0.342	1.594
3d	167.741	30.576	129.836	30.677	0.370	1.632
3e	167.227	33.197	133.409	33.197	0.400	1.677
3f	166.671	33.957	134.275	33.961	0.409	1.687
MBZ	179.483	-12.039	90.430	6.708	0.081	1.136
Trolox	159.057	-13.367	77.974	5.129	0.062	0.980
Vitamin-c	195.245	-6.126	104.268	9.709	0.117	1.310
Resveratrol	159.200	8.282	97.769	14.028	0.169	1.229
Quercetin	182.574	45.728	160.848	46.697	0.563	2.021

In the water-phase DAM (**Figure 4b**) for the reference compounds and antioxidants, it shows that most amidic compounds **1**(**a**-**f**)-3(**a**-**f**), thioethers (**I**-**III**), and **MBZ** are in the right antioxidant sector, being suitable electron donors. This variation in the result is due to the change in the solvent used, in which the presence of water promotes the donation of electrons, directly modifying the antiradical and antioxidant activity. In the case of DMSO phase DAM (**Figure 4c**), small molecules (**MBZ** and thioethers **I**-**III**) and amidic derivatives with saturated chains (**1a**-**3a**) are found in the right antioxidant sector. While the other amidic derivatives **1**(**b**-**f**)-**3**(**b**-**f**) are in the zone of bad antiradical showing a bad donation or acceptance of electrons. These results are like those shown in the gas-phase, in addition to agreeing with the results of antioxidant assays ($DPPH^{\bullet}$ and $ABTS^{\bullet+}$), which confirm that **MBZ**, thioethers (**I**-**III**) present a higher percentage of antioxidant activity. In the pentyl ethanoate phase DAM (**Figure 4d**) for the reference compounds and antioxidants, they show as in the water phase that most amidic compounds **1**(**a**-**f**)-**3**(**a**-**f**), thioethers (**I**-**III**) and **MBZ** are in the right antioxidant sector, being suitable donors of

electrons. The similarity of the results in the phases water and pentyl ethanoate can be related to the physiological conditions, which could have the same behavior in the living organisms.

Electrophilicity (ω)

The electrophilicity was calculated in different phases (gas; water; DMSO and pentyl ethanoate) for MBZ-derived compounds (thioethers and amides) and reference antioxidants are shown in **Figure 5**. On the contrary to the DAM, electrophilicity is not linearly dependent on ionization energy (IE). In fact, for compounds with a very low IE, the electrophilicity values increase. Moreover, for a species to be considered as antiradical, it must have low electrophilicity values. Since, in a chemical reaction involving two reactants, the one with the lowest electrophilicity value is expected to act as nucleophile [47]. According to the values obtained in this study, the compounds that present low electrophilicity values in all the phases studied are **MBZ**, **I-III**, and **1a-3a**, which compete with the reference antioxidants (Trolox and vitamin C) being the most promising to deactivate free radicals using the SET mechanism. The results obtained coincide with those shown in the DAM (DMSO phase) and the antioxidant assays ($DPPH^{\bullet}$ and $ABTS^{\bullet+}$) confirming that these compounds have a high probability of presenting good antiradical activity.

Journal Pre-proof

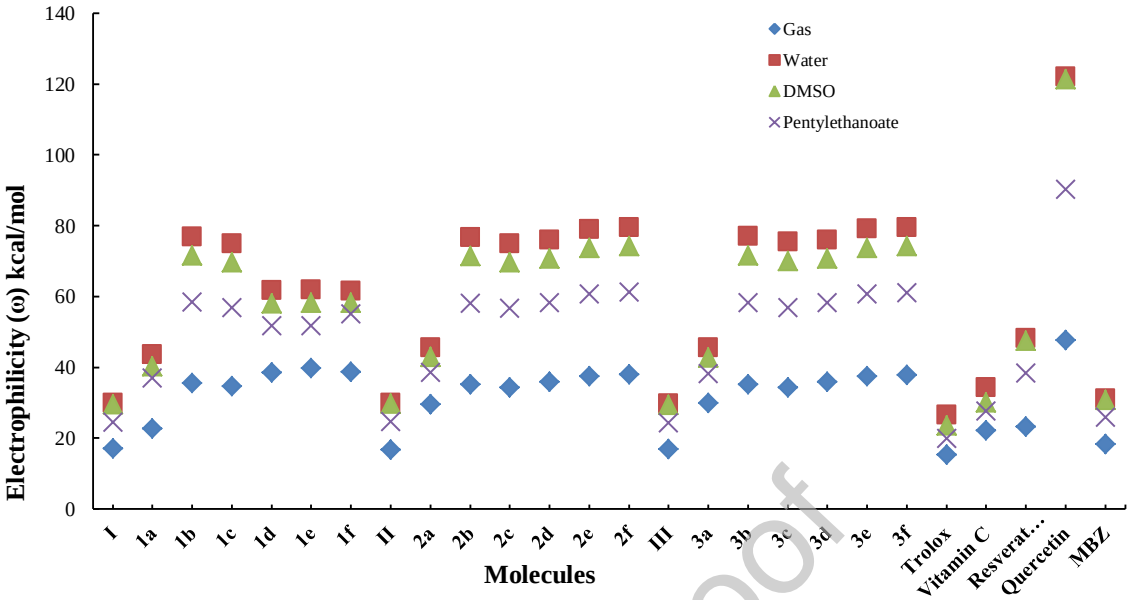

Figure 5. Electrophilicity of the synthesized compounds and some antioxidants used as references.

Journal Pre-proof

Descriptive QSAR

QSAR Molecular properties and topological descriptors of the synthesized compounds **1(a-f)-3 (a-f)** were calculated in **SPARTAN'14 V1.1.0** [48] and **DRAGON**® [49] based on the structures previously optimized geometrically by DFT (**Table 3**). The parameters calculated to perform the DAM in DMSO were included in the set of molecular descriptors as well. Genetic algorithm used in MobyDigs® software results showed that the synthesized compounds have sufficient affinity to be able to integrate the QSAR % Scavenging **ABTS**$^{\bullet+}$ study except for compounds **1f** and **2f** since the presence of bromine in the structure causes more factors to affect the antiradical capacity than in the rest of the molecules. The Linear relation of calculated Log % Scavenging **ABTS**$^{\bullet+}$ versus Log

experimental activity is shown in **Figure 6**. The best mathematical model, according to all the statistical parameters, is shown below.

Log% Scav. **ABTS$^{\bullet+}$**$_{CAL}$= 0.014 [VOLUME] + 0.062 [Ss] - 0.012 [CSI] - 0.635 [Ra_{DMSO}] - 1.58

R^2 = 83.97 Q^2_{LOO} = 61.95 s = 0.08 F = 11.8

ΔK = 0.041 (0) ΔQ = 0.006 (- 0.005) R^P= 0.119 (0.10) RN = -0.182 (-0.239)

Table 3. Molecular Descriptors used in the ABTS$^{\bullet+}$ QSAR Model Assay, Experimental and Calculated Log% Scavenging.

Comp.	Volume (Å^3)	Ss	CSI	R_aD	Log % Scav. Exp.	Log % Scav. Cal.
1a	310.38	45.17	395	0.192	0.602	0.704
1b	309.51	46.17	395	0.437	0.699	0.598
1c	306.2	47.17	395	0.419	0.602	0.625
1d	305.3	53.83	447	0.288	0.477	0.485
1e	314.17	49.94	447	0.291	0.477	0.366
2a	328.8	46.67	416	0.179	0.903	0.811
2b	327.95	47.67	416	0.435	0.778	0.698
2c	324.63	48.67	416	0.419	0.699	0.724
2d	323.92	55.33	470	0.430	0.477	0.472
2e	333.15	51.44	470	0.455	0.301	0.345
3a	347.12	48.17	456	0.179	0.699	0.680
3b	345.26	49.17	456	0.437	0.477	0.553
3c	343.06	50.17	456	0.423	0.699	0.593
3d	342.63	56.83	514	0.430	0.301	0.299

Journal Pre-proof

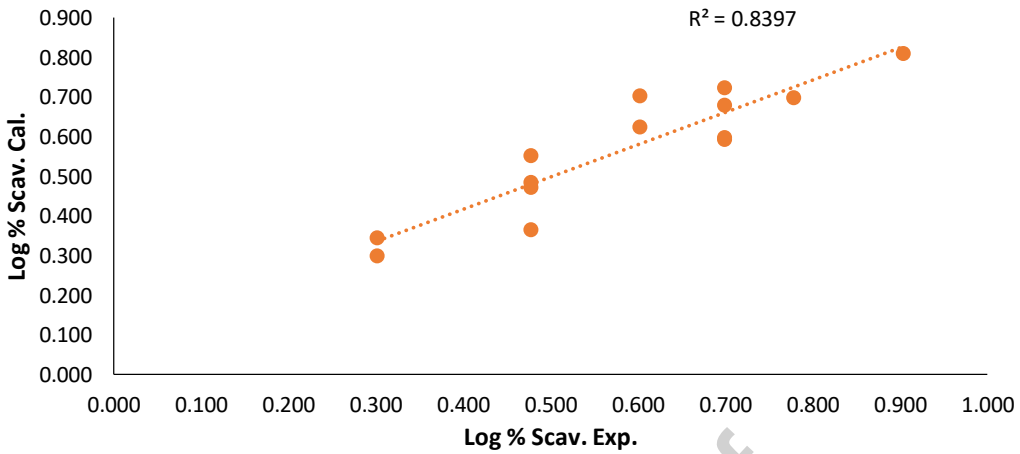

Figure 6. Linear relation of calculated Log % Scavenging **ABTS**$^{\bullet+}$ *versus* Log experimental activity.

The analysis of the QSAR model indicates that the size and molecular shape are relevant for the antiradical activity, since the higher the possibility of interaction with ABTS increases. The descriptor Ss (Sum of Kier-Hall electropological states) in some way confirms this relationship since it represents the intrinsic electronic state of each atom of the molecule (E-State) as a radius of electronegativity and the summation occurs throughout the structural skeleton of σ bonds, increasing the higher number of atoms in the molecule and with it the overall electronegativity [50, 51]. CSI (Eccentric Connectivity Index) is a numerical topological descriptor of the molecular structure derived from the corresponding distance-proximity graph and has been used successfully in numerous QSPR / QSAR studies of biological activities since it has the tremendous discriminatory capacity [52]. The presence of this descriptor with a negative sign in the model indicates that the molecular structures of the most abundant synthesized compounds have a smaller value of this topological index, as occurs with some polymers and their analogs with more complex

structures [53]. The electron acceptance index calculated for DMSO medium (Ra_{DMSO}) appears in the mathematical model with a negative sign and indicates that the lower this value, the easier it is to transfer an electron to accept it, coinciding with the concepts developed in the development of the Donor-Acceptor Map (DAM).

It should be noted that the QSAR % Scavengning **DPPH•** study could not be performed due to the low variability of the experimental data.

Conclusions

Compounds **I-III** and **1(a-f)-3(a-f)** were synthesized and characterized by NMR of ^{1}H, ^{13}C NMR, IR, and elemental analysis. In the antioxidant assay, DPPH● **MBZ** was the compound with the highest activity to inhibit 73% of the radical DPPH●, showing better radical entrapment than Trolox (reference antioxidant), showing only 70% inhibition. On the other hand, thioethers **I-III** showed moderate antiradical activity when presenting an inhibition percentage of 26, 18, and 3%, respectively. The insertion of alkyl groups in the exocyclic sulfur of **MBZ** in thioethers **I-III** causes a noticeable decrease in antioxidant activity. This effect was also observed in the lengthening of the substitute alkyl chain, where **III** showed a lower antiradical or antioxidant activity (5 µmol TE/L). According to the results of the antioxidant activity, the mechanism that best explains these results is the HAT, donating the thiol proton (S-H) since the raw material **MBZ** presented a high antiradical activity compared with the decreased activity of thioethers (**I-III**) and amide compounds **1(a-f)-3(a-f)**. In the case of DMSO phase DAM, **MBZ**, thioethers **I-III** and amide derivatives with saturated chain (**1a-3a**) are found in the right antioxidant sector. While **1(b-f)-3(b-f)** amide derivatives are in the wrong antiradical zone showing bad donation or acceptance of electrons. These results coincide with the results of the

Journal Pre-proof

antioxidant assays (DPPH● and ABTS●+), which confirm that **MBZ**, thioethers (**I-III**) present a higher percentage of antioxidant activity. Electrophilicity analysis shows the same trend as AMD, presenting **MBZ** compounds, thioethers **I-III,** and amides **1-3a** with higher antiradical activity. According to the QSAR study of the ABTS assay, the antiradical activity increases with the molecular size of the synthesized (unbrominated) compounds as well as a lower **Ra** value. According to the anti-radical mechanism of the proposed MBZ and the wide biological activity reported for this compound, a specific search for possible biological activities for this type of compounds would be interesting, by means of a detailed theoretical and experimental study.

Acknowledgments

Students OARR and JPMS thanks CONACYT for a Ph. D. scholarship 330102 and 330098, respectively. The authors also thank Universidad de Colima for the used infrastructure.

Credit Author Statement

- Omar Alejandro Ramos Rodríguez: Synthesis, Characterization, Antioxidant Activity and Writing.
- Juan Pablo Mojica Sánchez: DAM Analysis, Electrophilicity and Writing.
- José Antonio Valcárcel Gamiño: QSAR and Writing.

Journal Pre-proof

- Fernando Obledo Benicio and Carlos Eduardo Macías Hernández: Synthesis and Characterization.
- María Teresa Sumaya Martínez: Antioxidant Activity - Review.
- Francisco J. Martínez Martínez, Zeferino Gómez Sandoval and Ángel Ramos-Organillo: Synthesis, Characterization and DAM - Review & Editing.

Declaration of interests

☒ The authors declare that they have no known competing financial interests or personal relationships that could have appeared to influence the work reported in this paper.

☐The authors declare the following financial interests/personal relationships which may be considered as potential competing interests:

Journal Pre-proof

References

1. K. Anandarajagopal, R.N. Tiwari, K. Bothara, J.J. Sunilson, C. Dineshkumar, P. Promwichit, 2-Mercaptobenzimidazole Derivatives: Synthesis and Anticonvulsant Activity, Adv. Appl. Sci. Res., 1 (2010) 132-138.

2. R. M. Ahamed, S. F. Narren and A. S. Sadiq, synthesis of 2-mercaptobenzimidazole and some of its derivatives, J. AI-Nahrain University, 16 (2013) 77-83.

3. N. Jagerovic, M. L. Jimeno, I. Alkorta, J. Elguero and R. M. Claramunt, An experimental (NMR) and theoretical (GIAO) study of the tautomerism of benzotriazole in solution, Tetrahedron, 58 (2002), 9089-9094. https://doi.org/10.1016/S0040-4020(02)01157-2.

4. MV De Almeida, M. V. N. De Souza, S. H. Cardoso and J. V. De Assis, Synthesis of 2-mercaptobenzothiazole and 2-mercaptobenzimidazole derivatives condensed with carbohydrates as a potential antimicrobial agent, J. Sulfur Chem., 28 (2007), 17-22. https://doi.org/10.1080/17415990601055291.

5. K. Anandarajagopal, R. Tiwari, N. Venkateshan, G. Vinotha-Pooshan and P. Promwichit, Synthesis and characterization of 2-mercaptobenzimidazole derivatives as potential analgesic agents, J. Chem. Pharm. Res., 2 (2010), 230-236.

6. H. Gurer-Orhan, H. Orhan, S. Suzen, M. O. Püsküllü and E. Buyukbingol, Synthesis and evaluation of in vitro antioxidant capacities of some benzimidazole derivatives, J. Enzyme Inhib. Med. Chem., 21 (2006), 241–247. https://doi.org/ 10.1080/14756360600586031.

7. S. Rajasekaran, G. Rao and A. Chatterjee, Synthesis, Anti-Inflammatory and Antioxidant activity of some substituted Benzimidazole Derivatives, Int. J. Drug. Dev. & Res., 4 (2012), 303-309.

8. A. Y. Bespalov, T. L. Gorchakova, A. Y. Ivanov, M. A. Kuznetsov, L. M. Kuznetsova, A. S. Pankova and M. S. Avdontceva, Alkylation and Aminomethylation of 1,3-Dihydro-2H-Benzimidazole-2-Thione, Chem. Heterocycl. Compd., 50 (2015), 1547-1558. https://doi.org/ 10.1007/s10593-014-1623-z.

9. T. Rebstock, C. Ball, C. Hamner and H. Sell, Effect of chemical structure on the growth inhibition of plants with some acid analogs of 2-mercaptobenzimidazole, J. Article, 19 (1955) 382-384.

10. M. Salman, M. Abu-Krisha and H. El-Sheshtawy, Charge Transfer Complexes of MBI with α-and Π-Electron Acceptor, Cand. J. Analy. Sci. Spect., 49 (2004), 282-289.

Journal Pre-proof

11. D. Saxena, R. Kajuria, O. Suri, Synthesis and Spectral Studies of 2-Mercaptobenzothiazole Derivatives, J. Hetro. Chem., 19 (1982), 681-685.

12. S. Berchmans, S. Arivukkodi and N. Yegnaraman, Self-assembled monolayers of 2-mercaptobenzimidazole on gold: stripping voltammetric determination of Hg(II), Electro. Commun., 2 (2000), 226-229. https://doi.org/ 10.1016/S1388-2481(00)00002-3.

13. K. Chalapathi, L. Rameshbabu, P. Madhu and G. Maddaiah, 2-Mercaptobenzimidazole Immobilized with Amberlite Xad-2 Using as Solid Phase Extractor for the Determination of Fe(II), Cu(II), and Cd(II) in Sewage and Waste Water Samples by Flame Atomic Absorption Spectrometry, Adv. Appl. Sci, Res., 1 (2010), 27-35.

14. O. Temiz-Arpaci, T. Coban, B. Tekiner-Gulbas, B. Can-Eke, I. Yildiz, E. Aki-Sener, I. Yalcin and M. Iscan, A study on the antioxidant activities of some new benzazole derivatives, Acta Biol. Hung., 57(2006), 201-209. https://doi.org/ 10.1556/ABiol.57.2006.2.7.

15. S. S. Chhajed and C. D. Upasani, Synthesis and Antioxidant Activity of Some Novel 2-Substituted Analogues of Benzimidazoles, J. Pharm. Res., 4 (2011), 340-343.

16. A. Martínez, Donator Acceptor Map of Psittacofulvins and Anthocyanins: Are They Good Antioxidant Substances?, J. Phys. Chem. B., 113 (2009), 4915-4921. https://doi.org/ 10.1021/jp8102436.

17. Y. Yu, F. Fan, D. Wu, C. Yu, Z. Wang, & M. Du, Antioxidant and ACE inhibitory activity of enzymatic hydrolysates from Ruditapes philippinarum, Molecules, 23 (2018), 1189. https://doi.org/10.3390/molecules23051189.

Journal Pre-proof

18. M. Reina, R. Castañeda-Arriaga, A. Perez-Gonzalez, E. G. Guzman-Lopez, D. X. Tan, R, J, Reiter, & A. Galano, A computer-assisted systematic search for melatonin derivatives with high potential as antioxidants, Melatonin Research, 1 (2018), 27-58. https://doi.org/10.32794/mr11250003.

19. J. R. Johns and J. A. Platts, Theoretical insight into the antioxidant properties of melatonin and derivatives, Org. Biomol. Chem., 12 (2014), 7820-7827. https://doi.org/ 10.1039/c4ob01396d.

20. J. L. Gazquez, A. Cedillo and A. Vela, Electrodonating and Electroaccepting Powers, J. Phys. Chem. A, 111 (2007), 1966-1970. https://doi.org/10.1021/jp065459f.

21. A. Martínez, Donator−Acceptor Map and Work Function for Linear Polyene-Conjugated Molecules. A Density Functional Approximation Study, J. Phys. Chem. B, 113 (2009), 3212-3217. https://doi.org/10.1021/jp8106364.

22. A. Martínez, R. Vargas and A. Galano, What is Important to Prevent Oxidative Stress? A Theoretical Study on Electron-Transfer Reactions between Carotenoids and Free Radicals, J. Phys. Chem. B, 113 (2009), 12113-12120. https://doi.org/10.1021/jp903958h.

23. A. Galano, Relative Antioxidant Efficiency of a Large Series of Carotenoids in Terms of One-Electron Transfer Reactions, J. Phys. Chem. B, 111 (2007), 12898-12908. https://doi.org/10.1021/jp074358u.

24. A. Martínez, M. A. Rodríguez-Gironés, A. Barbosa and M. Costas, Donator acceptor map for carotenoids, melatonin and vitamins. J. Phys. Chem. A, 112 (2008), 9037-9042. https://doi.org/10.1021/jp803218e.

Journal Pre-proof

25. A. Martínez, Donator Acceptor Map of Psittacofulvins and Anthocyanins: Are They Good Antioxidant Substances?, J. Phys. Chem. B., 113 (2009), 4915-4921. https://doi.org/ 10.1021/jp8102436.

26. D. A. Hernandez, J.G. Rodriguez-Zavala & F. J. Tenorio, DFT study of antioxidant molecules from traditional Japanese and Chinese teas: comparing allylic and phenolic antiradical activity, J. Struct. Chem., 31 (2020), 359-369. https://doi.org/10.1007/s11224-019-01411-z.

27. D.O Kim, K.W. Lee, H.J. Lee, C.Y. Lee, Vitamin C Equivalent Antioxidant Capacity (VCEAC) of Phenolic Phytochemicals, J. Agric. Food Chem. 50 (2002) 3713-3717. https://doi.org/10.1021/jf020071c.

28. R. Re, N. Pellegrini, A. Proteggente, A. Pannala, M. Yang, C. Rice-Evans, Antioxidant activity applying an improved ABTS radical cation decolorization assay, Free Radic. Biol. Med. 26 (1999) 1231-1237. https://doi.org/10.1016/S0891-5849(98)00315-3.

29. M.T. Sumaya-Martínez, S. Cruz-Jaime, E. Madrigal-Santillán, J.D. García-Paredes, R. Cariño-Cortés, N. Cruz-Cansino, C. Valadez-Vega, L. Martinez-Cardenas, E. Alanís-García, Betalain, Acid Ascorbic, Phenolic Contents and Antioxidant Properties of Purple, Red, Yellow and White Cactus Pears, Int. J. Mol. Sci. 12 (2011) 6452-6468. https://doi.org/10.3390/ijms12106452.

30. M. J. Frisch, G. W. Trucks, H. B. Schlegel, G. E. Scuseria, M. A. Robb, J. R. Cheeseman, G. Scalmani, V. Barone, B. Mennucci, G. A. Petersson, H. Nakatsuji, M. Caricato, X. Li, H. P. Hratchian, A. F. Izmaylov, J. Bloino, G. Zheng, J. L. Sonnenberg, M. Hada, M. Ehara, K. Toyota, R. Fukuda, J. Hasegawa, M. Ishida, T. Nakajima, Y. Honda, O. Kitao, H. Nakai, T. Vreven, J. A. Montgomery, J. E.

Journal Pre-proof

Peralta, F. Ogliaro, M. Bearpark, J. J. Heyd, E. Brothers, K. N. Kudin, V. N. Staroverov, R. Kobayashi, J. Normand, K. Raghavachari, A. Rendell, J. C. Burant, S. S. Iyengar, J. Tomasi, M. Cossi, N. Rega, J. M. Millam, M. Klene, J. E. Knox, J. B. Cross, V. Bakken, C. Adamo, J. Jaramillo, R. Gomperts, R. E. Stratmann, O. Yazyev, A. J. Austin, R. Cammi, C. Pomelli, J. W. Ochterski, R. L. Martin, K. Morokuma, V. G. Zakrzewski, G. A. Voth, P. Salvador, J. J. Dannenberg, S. Dapprich, A. D. Daniels, O. Farkas, J. B. Foresman, J. V. Ortiz, J. Cioslowski and D. J. Fox, Gaussian 09, Revision A.02, Gaussian, Inc., Wallingford CT, 2016.

31. A. D, Becke, Density-functional exchange-energy approximation with correct asymptotic behavior, Phys. Rev. A, 38 (1988), 3098. https://doi.org/10.1103/PhysRevA.38.3098.

32. J. P. Perdew and Y. Wang, Accurate and simple analytic representation of the electron-gas correlation energy, Phys. Rev. B, 45 (1992), 13244–13249. https://doi.org/10.1103/PhysRevB.45.13244.

33. M. P. Andersson and P. Uvdal, New Scale Factors for Harmonic Vibrational Frequencies Using the B3LYP DensityFunctional Method with the Triple-ζ Basis Set 6-311+G (d,p), J. Phys. Chem. A, 109 (2005), 2937–2941. https://doi.org/10.1021/jp045733a.

34. S. Lahmidi, M. El Hafi, M. Boulhaoua, A. Ejjoummany, M. El Jemli, E. M. Essassi & J. T. Mague, Synthesis, X-ray, spectroscopic characterization, DFT and antioxidant activity of 1, 2, 4-triazolo [1, 5-a] pyrimidine derivatives, J. Mol. Struct., 1177 (2020), 131-142. https://doi.org/10.1016/j.molstruc.2018.09.046.

Journal Pre-proof

Journal Pre-proof

35. S. M. Reza Nazifi, M. H. Asgharshamsi, M. M. Dehkordi & K. K. Zborowski, Antioxidant properties of Aloe vera components: a DFT theoretical evaluation, Free Radic. Res., 53 (2019), 922-931. https://doi.org/10.1080/10715762.2019.1648798.

36. A. V. Marenich, C. J. Cramer and D. G. Truhlar, Universal Solvation Model Based on Solute Electron Density and on a Continuum Model of the Solvent Defined by the Bulk Dielectric Constant and Atomic Surface Tensions, J. Phys. Chem. B, 113 (2009), 6378–6396. https://doi.org/10.1021/jp810292n.

37. V. Chahal & R. Kakkar, Theoretical study of the structural features and antioxidant potential of 4-thiazolidinones, J. Struct. Chem., (2020), 1-10. https://doi.org/10.1007/s11224-020-01517-9.

38. R. G. Parr, L. V. Szentpály and S. Liu, Electrophilicity Index, J. Am. Chem. Soc., 121 (1999), 1922–1924. https://doi.org/10.1021/ja983494x.

39. B. Neises and W. Steglich, Simple Method for the Esterification of Carboxylic Acids, Angewandte Chem. Int., 17 (1978), 522-524. https://doi.org/10.1002/anie.197805221.

40. J.M. Berger, R. J. Rana, H. Javeed, I. Javeed and S. L. Schulien, Radical Quenching of 1,1-Diphenyl-2-picrylhydrazyl: A Spectrometric Determination of Antioxidant Behavior, J. Chem. Educ., 85 (2008), 408-410. https://doi.org/10.1021/ed085p408.

41. R. L. Prior, X. Wu and K. Schaich, Standardized methods for the determination of antioxidant capacity and phenolics in foods and dietary supplements, J. Agric. Food Chem., 53 (2005), 4290-4302. https://doi.org/10.1021/jf0502698.

42. E. T. Denisov and I. V. Khudyakov, Mechanisms of action and reactivities of the free radicals of inhibitors, Chem. Rev., 87 (1987), 1313-1357. https://doi.org/10.1021/cr00082a003.

43. C. Avendaño, Introduction to Pharmaceutical Chemistry 2ed. Drug design based on free radical chemistry. Antioxidant therapy, (2015), 15-22.

44. S. F. Barbuceanu, D. C. Ilie, G. Saramet, V. Uivarosi, C. Draghici & V. Radulescu, Synthesis and antioxidant activity evaluation of new compounds from hydrazinecarbothioamide and 1,2,4-triazole class containing diaryl sulfone and 2,4-difluorophenyl moieties, Int. J. Mol. Sci., 15 (2014), 10908-10925. https://doi.org/10.3390/ijms150610908.

45. D. Huang, B. Ou, and R. L. Prior, The chemistry behind antioxidant capacity assays, J. Agric. Food Chem., **53** (2005), 1841-1856. https://doi.org/10.1021/jf030723c.

46. M. Ozgen, R. N. Reese, A. Z. Tulio, J. C. Scheerens, and A. R. Miller, Modified 2,2-Azino-bis-3-ethylbenzothiazoline-6-sulfonic Acid (ABTS) Method to Measure Antioxidant Capacity of Selected Small Fruits and Comparison to Ferric Reducing Antioxidant Power (FRAP) and 2,2 '-Diphenyl-1-picrylhydrazyl (DPPH) Methods, J. Agric. Food Chem., 54 (2006), 1151-1157. https://doi.org/10.1021/jf051960d.

47. M. Reina, R. C. Arriaga, A. P. González, E. G. Guzmán, D. X. Tan, R. J. Reiter and A. Galano, A computer-assisted systematic search for melatonin derivatives with high potential as antioxidants, Melatonin Research, 1 (2018), 27-58. https://doi.org/10.32794/mr11250003.

48. PC SPARTAN pro Molecular Modeling for the Desktop, Chem. & Eng. News Archive, 77 (1999), 2.

49. R. Todeschini, V. Consonni, A. Mauri, M. Pavan, Detecting "bad" regression models: multicriteria fitness functions in regression analysis, Anal Chim Acta., 1 (2004),199-208. https://doi.org/10.1016/j.aca.2003.12.010.

Journal Pre-proof

Journal Pre-proof

50. L. H. Hall and L. B. Kier, Electrotopological State Indices for Atom Types: A Novel Combination of Electronic, Topological, and Valence State Information, J. Chem. Inf. Comput. Sci., 35 (1995), 1039-1045. https://doi.org/10.1021/ci00028a014.

51. NS. Sapre, N. Pancholi, S. Gupta, N. Sapre. Computational modeling of tetrahydroimidazo-[4,5,1-jk][1,4]-benzodiazepinone derivatives: an atomistic drug design approach using Kier-Hall electrotopological state (E-state) indices, J. Comp. Chem., 29 (2008), 1699-1706. https://doi.org/10.1002/jcc.20931.

52. S.Gupta, M. Singh and A.K.Madan, Application of Graph Theory: Relationship of Eccentric Connectivity Index and Wiener's Index with Anti-inflammatory Activity, J. of Math. Anal and App., 266 (2002), 259-268. https://doi.org/10.1006/jmaa.2000.7243.

53. V. Sharma, R. Goswami and A. K. Madan, Eccentric Connectivity Index: A Novel Highly Discriminating Topological Descriptor for Structure−Property and Structure−Activity Studies, J. Chem. Inf, Comput. Sci, 37 (1997), 273-282. https://doi.org/10.1021/ci960049h.

Journal Pre-proof

GRAPHICAL ABSTRACT

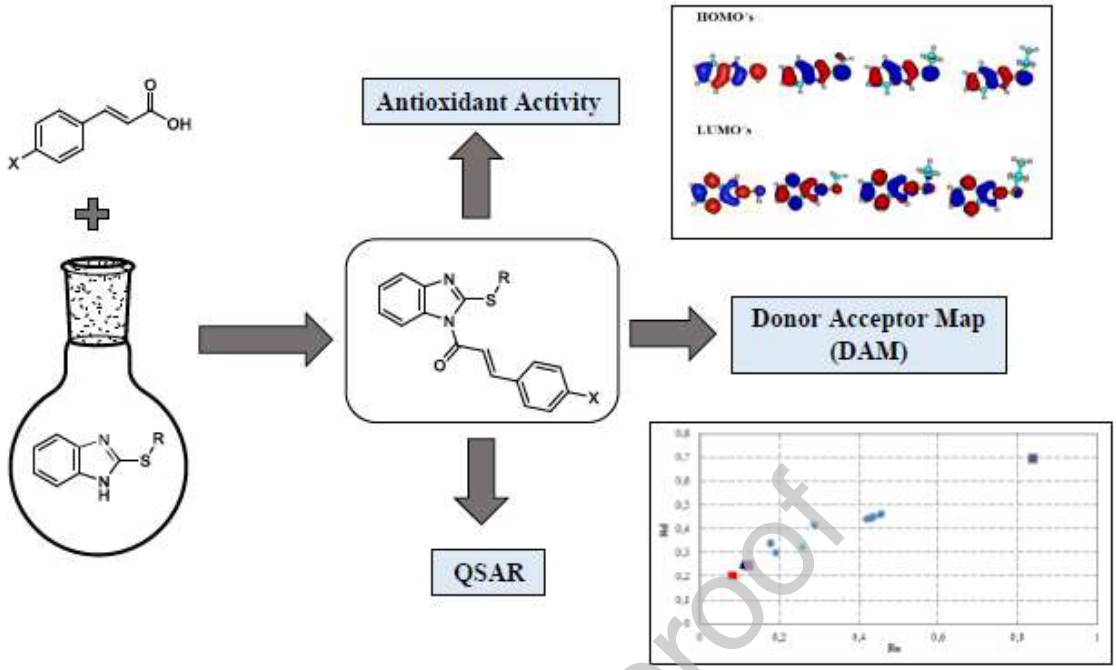

Journal Pre-proof